A thermal analysis on self-propagating high temperature synthesis in joining technology

T. Fiedler*, I.V. Belova, S. Broxtermann and G.E. Murch

University Centre for Mass and Thermal Transport in Engineering Materials
Priority Research Centre for Geotechnical and Materials Modelling
School of Engineering, The University of Newcastle
Callaghan, NSW 2308, Australia

*corresponding author: E-mail: Thomas.Fiedler@Newcastle.edu.au,
phone: +61 2492 16208, fax: +61 2492 16946.

Abstract This paper addresses the thermal analysis of self-propagating high temperature synthesis (SHS) in joining operations of temperature sensitive materials. A parametric Finite Element analysis of SHS is conducted, i.e. the influence of reaction rate, ignition temperature and reaction zone thickness on reaction stability and velocity is investigated. Special regard is given to surrounding materials such as amorphous alloys in joining operations. These materials act as heat sinks that conduct energy away from the reaction zone and thus diminish or even extinguish the reaction. In addition to the numerical simulation, analytical relations are developed to introduce criteria for reaction stability. Analytical and numerical results are compared for verification.

Keywords: Thermal analysis; SHS; Amorphous alloy; NiAl; Finite element analysis; Analytical

1. Introduction

The focus of this paper is the application of self-propagating high temperature synthesis (SHS) to the joining of solids. This type of reaction constitutes a highly transient thermal diffusion problem: the heat that is generated by the reaction is simultaneously conducted away from the reaction zone. The conductive heat flux increases local temperatures in adjacent areas and thus provides the activation energy to propagate the reaction. The velocity of the reaction front generally increases with the thermal diffusivity of the materials. However, high diffusivities also mean fast energy dissipation with the effect that temperatures inside the reaction zone may decrease below the ignition temperature resulting in extinction of the reaction. In this case, the reaction is no longer self-propagating. The present paper aims to define criteria for the stability of SHS and to develop simple relations to estimate the velocity of the reaction front.

SHS reactions are very fast reactions that upon ignition emit a sufficiently large amount of heat to maintain the reaction but where the reactants and products remain in the condensed state [1]. SHS reactions may be conveniently divided into two main classifications that are distinguished by the mode of ignition. In ‘simultaneous mode’, the SHS reaction is initiated through simultaneous heating of the reactants to the inherent SHS ignition temperature T_{Ig} at which point the entire sample uniformly reacts. In this mode, the reaction can in principle be very well controlled because heat is evolved uniformly through the sample. In ‘propagating mode’ on the other hand, the SHS reaction is conveniently initiated through very localised heating of the sample (usually by a spark) at which point the reactants are elevated to T_{Ig} and an exothermic combustion front is generated. The present paper

focuses exclusively on the propagating mode. The propagating front heats the next adjacent layer of reactants and hence promotes a similar temperature increase and reaction event and so on. By changing the reactants, the thickness of the individual layers and the number of layers, then the flame velocities, temperatures and heat evolved by the reaction can be manipulated so that in principle a reactive foil can be used as a precisely controlled local heat source for the purposes of joining metallic materials [2]. Since the total heat released is actually quite small, a reactive foil is believed to be particularly well suited for joining temperature-sensitive components such as microelectronics components and amorphous alloys thus avoiding the need for solid state diffusion-bonding or conventional welding or brazing, all of which are unsuitable for joining such materials [2,3]. If the cooling rate is too slow, crystallization results and is accompanied by a pronounced degradation of the unique properties of amorphous alloys. Amorphous alloys can be joined by friction and pulse current techniques but these techniques are restricted in practice to very limited joint geometries [4]. Amorphous alloys are very promising materials for many engineering applications because of their extraordinary properties that can include a very high tensile strength (typically ~2 GPa), high fracture toughness (typically ~20 $MPa \cdot m^{1/2}$), high corrosion resistance and soft magnetic properties [5]. It is generally acknowledged [5] that the lack of a well-controlled and general means of joining amorphous alloys is significantly restricting their employment in many engineering applications. The present paper aims to advance knowledge for the joining of amorphous alloys by making use of self-propagating high temperature synthesis (SHS) reactions.

SHS in joining operations has been considered by Hu et al. [6]. A copper-based welding material was tested for suitability in the emergency welding of thin metal sheets. The focus of the paper was the mechanical characterisation of the bond and a tensile strength of approximately 200 MPa was found. In Pascal et al. [7] SHS joining with nickel monoaluminide (NiAl) was considered. After the pre-heating of the joining couple to 920 K, the exothermic reaction synthesis was initiated which then propagated along the NiAl powder compact. Maximum temperatures of 1950 K which corresponds to the melting point of NiAl were observed. Due to the high temperatures, the adjacent substrate was melted inside a 100 μm thick layer. In Gunduz et al.[8] numerical simulations on SHS of nanoscale nickel-aluminium multilayers were conducted. A two-stage reaction was assumed where the rapid growth of Ni_2Al_3 is followed by the formation of NiAl at elevated temperatures. Good agreement with experimental temperature and front velocity data was found. Rabinovich and colleagues [9] investigated the conditions for combustion synthesis of Ni and Al on a glass substrate. Their model simulated the propagation of the synthesis as well as the accompanying thermal wave into the substrate. A minimum number of bi-layers (i.e. a minimum reaction zone thickness) were identified in order to obtain stable self-propagation of the reaction. Levchenko and colleagues [10] considered a different topology of the same reaction where Ni nanoparticles were coated with Al. Molecular dynamics simulations indicated a highly exothermic reaction at ignition temperatures as low as 200 K.

The present paper focuses on the application of SHS in joining technology of temperature sensitive materials such as amorphous alloys. Within this context, SHS must generate sufficient thermal energy to self-propagate but at the same time, the transfer of thermal energy to the adjacent amorphous alloys must be minimised in order to avoid crystallization of the material. Analytical criteria for minimum reaction rates are developed and compared to numerical finite element simulations. A systematic parametric study of SHS is conducted. To this end, the reaction parameters reaction rate, reaction zone thickness and ignition temperature are considered. Furthermore, the impact of different material properties, i.e. amorphous alloys on SHS is investigated. Finally, transient temperature profiles inside amorphous alloys are calculated in order to evaluate the thermal impact of the joining process.

2. Finite Element Modelling

For the numerical analysis, the finite element (FE) method is used. As a starting point we select the basic form of the heat transfer equation

$$\rho \cdot C \cdot \frac{\partial T}{\partial t} + \left(\frac{\partial q_x}{\partial x} + \frac{\partial q_y}{\partial y} + \frac{\partial q_z}{\partial z} \right) = Q\,, \tag{1}$$

where ρ is the density, C is the heat capacity, q_i are the components of the heat flow per unit area and Q is the inner heat-generation rate per unit volume. Equation (1) is an energy balance that relates the change in internal energy to energy flow and energy generation. Using Fourier's law, the heat flow components can be written as:

$$q_\mathrm{i} = -\lambda \cdot \frac{\partial T}{\partial i}\,,\ \ i = x, y, z\,, \tag{2}$$

where λ is the thermal conductivity. For use in finite element (FE) analysis, a discretised form of Eq. (1) is obtained after the subsequent application of the Galerkin method and the divergence theorem:

$$\mathbf{C}(T) \cdot \frac{d\mathbf{T}}{dt} + \mathbf{K}(T) \cdot \mathbf{T} = \mathbf{Q}\,. \tag{3}$$

In this notation, the matrix $\mathbf{C}(T)$ contains temperature-dependent heat capacities and $\mathbf{K}(T)$ is the thermal conductivity matrix. The column matrix $\mathbf{Q}$ contains the nodal heat fluxes of the discretised geometry. The discretisation with respect to time is achieved using the backward difference scheme [11]:

$$\left[\frac{1}{\Delta t} \cdot \mathbf{C}(T) + \mathbf{K}(T) \right] \cdot \mathbf{T}_n = \mathbf{Q}_n + \frac{1}{\Delta t} \cdot \mathbf{C}(T) \cdot \mathbf{T}_{n-1}\,. \tag{4}$$

Eq. (4) allows the calculation of nodal temperature for each time increment Δt. In the present FE computations, a volume heat flux boundary condition R (unit W/m^3) is used to simulate the heat generation of the chemical reaction. The volume flux is converted into a nodal heat flux $Q_n = R \cdot V$ (Unit W), where V is the element volume divided by the number of element nodes (i.e. the volume assigned to each node, unit m^3).

A schematic of the FE calculation model is shown in Fig. 1. Two reactants A and B are brought into contact at the initial temperature T_In. At their interface, a reaction zone with the thickness l is defined. A simplified reaction model is used where the reaction is initiated at the ignition temperature T_Ig. Below this threshold, the reaction ceases and no heat is generated. The rate of energy generation R of the reaction is defined per unit volume (units: kW·mm^{-3}) and is an important parameter for the characterization of SHS. In order to initiate the reaction, a small fraction of the reaction zone is preheated to a temperature $T_\mathrm{S} > T_\mathrm{Ig}$ simulating an igniting spark. Preliminary analysis was conducted in order to ensure that reaction stability and velocity are independent of the spark energy. The thickness l of the reaction zone can be increased, for example by stacking multiple layers of nano-foils of reactants. Inside the reaction zone sufficient amounts of reactants are encountered so that reaction can occur. The exothermic reaction causes the release of thermal energy resulting in a local temperature increase. Due to thermal conduction, the ignition temperature in the adjacent reaction zone is reached and the reaction front (coordinate L) propagates. The velocity of the reaction front is calculated according to the differential $v = \mathrm{d}L / \mathrm{d}t$. The material above and below the reaction zone is considered large enough so that no edge effects occur, i.e. beyond a critical distance the material always remains at its initial temperature. In joining applications, these thermal reservoirs correspond to the components to be joined, for example bulk amorphous alloys.

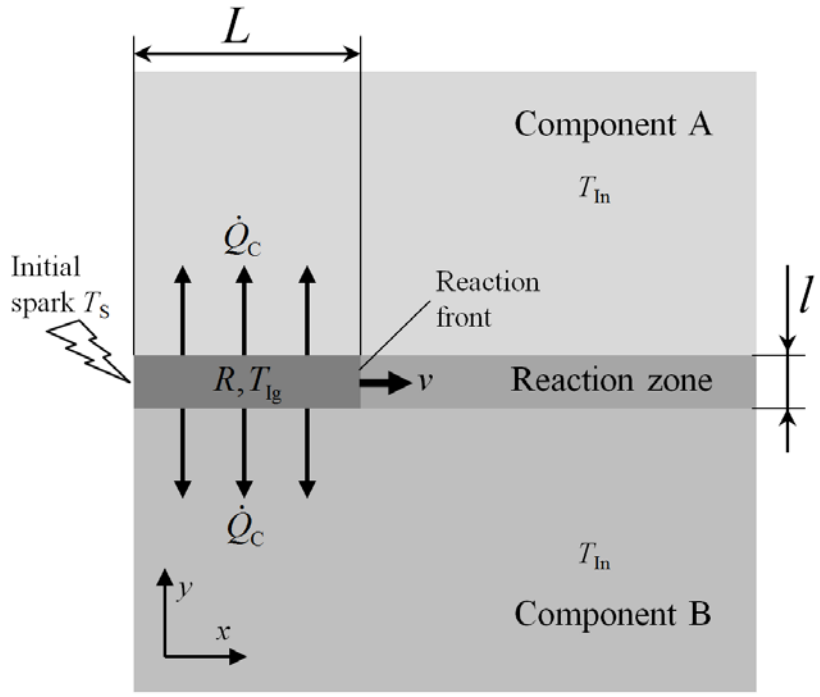

Fig. 1 Calculation model

In order to control the complexity of the analysis, the following simplifications are introduced. First, the material properties of components A and B are identical, i.e. two components of the identical material are joined. This approach allows a parametric study of the reaction behaviour for different joining materials. Second, the material properties of components and reaction zone are temperature-independent. Finally, the reaction rate R is constant above, and zero below, the ignition temperature T_{Ig}. It should be mentioned here that the results of the numerical analysis depend only on material and reaction parameters but are independent of the details of the reaction. However, the standard reaction parameters of this study are derived from the important reaction of Ni and Al to form NiAl. Accordingly, the material properties of the reaction zone correspond to NiAl (see Table 1). Typical ignition temperatures of blended nano-powders are in the range of 590 K to 690 K [12] and as low as 200 K for Ni-coated aluminium particles [13]. Furthermore, the reaction enthalpy of the NiAl formation is 0.61 eV / atom (i.e. 4.16 J·mm^{-3}) [13].

For the Finite Element calculations, planar four-noded isoparametric elements with bilinear interpolation were used. Mesh-refinement analysis indicates a minimum element density of 100 elements / mm^2 in order to ensure numerical convergence. The system is adiabatic, i.e. no heat transfer between the finite element model and the surroundings occurs. As mentioned above, the finite element model is chosen large enough so that no temperature change at the upper and lower edges (see Fig. 1) can be observed. All elements exhibit an initial temperature of 300 K unless mentioned otherwise. A small fraction of the reaction zone is preheated to T_{Ig} = 2000 K in order to simulate the initiating spark. A preliminary study showed that the spark energy has a minor impact on the initial velocity of the reaction. In order to eliminate this effect, the spark energy is minimised and the reaction front velocity is evaluated only after the reaction has stabilised. The evaluation of the reaction front velocity is performed using a user-defined subroutine. Nodal temperatures T_n are compared to the ignition temperature T_{Ig} at the end of each time increment. If the condition $T_n > T_{Ig}$ is fulfilled, the node lies within the reaction zone. The node with the maximum x coordinate describes the length L of the reaction zone (see Fig. 1) which is plotted versus time. The constant slope of this graph corresponds to the reaction front velocity v. The chemical reaction is simulated by a second user-defined subroutine. To this end, a nodal heat flux $Q_n = R \cdot V$ is activated if the following two conditions are fulfilled. First, the nodal temperature must exceed the ignition temperature $T_n > T_{Ig}$.

Second, the previously released energy $E_{\mathrm{n}} = \int Q_{\mathrm{n}} \mathrm{d}t / V$ must be smaller than the reaction enthalpy (i.e. reactants must still be available inside the nodal volume).

3. Criterion for Reaction Stability

In the following, the criteria for reaction stability are developed. Three different regimes are distinguished: stable, transient stable and unstable reaction. It will be shown that the reaction stability depends mainly on the reaction rate R per unit volume, the thermal conductivity λ and the thermal diffusivity D.

Stable reaction

Within the stable regime, reactions always self-propagate (i.e. propagate without the need of external energy after an initial spark). As a criterion, the steady state solution of Fourier's law is used. The amount of energy generated by the reaction $R \cdot V$ where V is the control volume must exceed the energy conducted away from the reaction zone. Since the reaction is surrounded by material on two sides, the conductive heat transfer loss must be considered in two directions:

$$R \cdot V \geq 2 \cdot \lambda \cdot A \cdot \frac{\Delta T}{\Delta x}. \tag{5}$$

The temperature difference ΔT is the initial reaction zone temperature T_{In} subtracted from the ignition temperature T_{Ig} and the spatial distance Δx is approximately half the thickness of the reaction zone l. The control volume V can be calculated according to $V = A \cdot l = l^3$ and accordingly Eq. (5) can be rewritten to:

$$R_{\mathrm{stat}} \geq 4 \cdot \lambda \cdot \frac{\left(T_{\mathrm{Ig}} - T_{\mathrm{In}}\right)}{l^2} \tag{6}$$

Transient stable reaction

Comparison with FE data (see Fig. 3) shows that Eq. (6) generally overestimates the minimum reaction rate for self-propagation. The explanation for this deviation is the pre-heating of the reaction zone due to adjacent reaction. As a consequence, the temperature difference ΔT is smaller than T_{Ig} - $T_{\mathrm{In.}}$ In order to include this effect, a second condition is introduced that describes a regime of transient stability. Transient stability means that a reaction is self-propagating under the condition that a fully developed temperature profile moves with a velocity v along the reaction zone.

For the purposes of estimating the minimum reaction rate R_{min}, let us assume a one-dimensional transient heat conduction problem where the reaction zone ($\geq T_{\mathrm{Ig}}$) is in contact with surrounding material at a lower temperature T_{In}. Under these conditions, the complementary error function can be used to describe the transient temperature profile in the region where $0 < x < L$ as:

$$T(y,t) = (T_{Ig}^{'} - T_{\mathrm{In}}) \cdot \mathrm{erfc}\left(\frac{y}{2\sqrt{D_y \cdot t}}\right) + T_{\mathrm{In}} \tag{7}$$

and in the region where $x > L$ as:

$$T(x,t) = (T_{Ig}^{'} - T_{\mathrm{In}}) \cdot \mathrm{erfc}\left(\frac{x}{2\sqrt{D_R \cdot t}}\right) + T_{\mathrm{In}} \tag{8}$$

where D_R is the thermal diffusivity of the reaction zone, D_y is the thermal diffusivity of the joining material, $T'_{Ig} = T_{Ig} + \varepsilon(T_{Ig} - T_{In})$ and ε determines the (minimum) amount of temperature increase above the ignition point necessary for the reaction to propagate (using this very simplistic model).

Accordingly, the time-dependent temperature difference between the reaction zone and neighbouring material (distance $l/2$, $0 < x < L$, use Eq. (8)) is:

$$\Delta T(t) = T(0,t) - T(l/2,t) \approx T_{Ig} - T(l/2,t) \tag{9}$$

Using Fourier's law, we can write that the conductive rate of heat transfer $\dot{Q}_C$ from the reaction zone towards the adjacent material is:

$$\dot{Q}_C(t) = \lambda \cdot A \frac{\Delta T(t)}{\Delta y} \approx 2 \cdot \lambda \cdot l \cdot \Delta T(t) \tag{10}$$

Again, the reaction term R (energy generated per volume) must be equal to or larger than the conductive rate of heat transfer (Eq. 10) in order to maintain the reaction. To avoid confusion with the static rate R_{stat} introduced in Eq. (6) the subscript tran(sient) is added:

$$R_{tran}(t) \geq \frac{2 \cdot \dot{Q}_C(t)}{V} \approx 4 \cdot \lambda \cdot \frac{\Delta T(t)}{l^2} \tag{11}$$

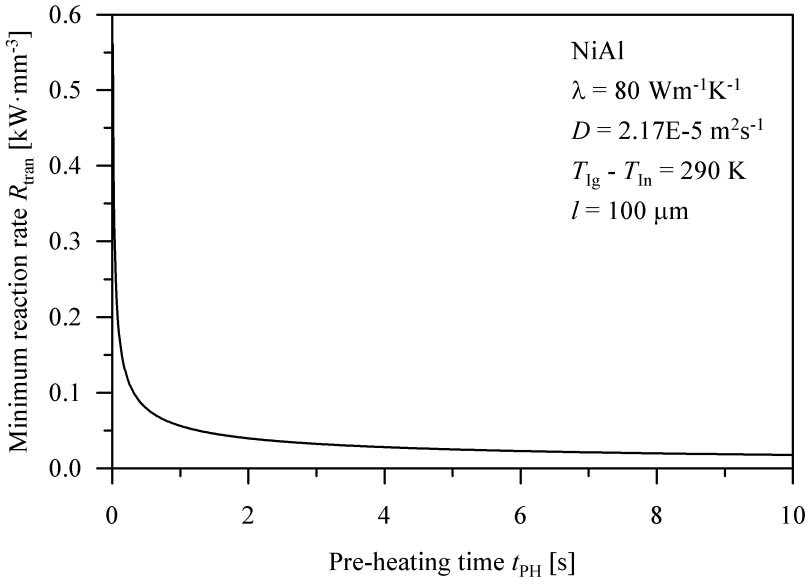

Fig. 2 Equation (11) plotted versus time.

Expression (11) is similar to the steady state condition (Eq. 6). However, the temperature difference is no longer constant but time dependent (see Eq. (9)). In Figure 2, the minimum required reaction rate R_{tran} is calculated using Eq. (11) and plotted versus the preheating time t_{PH}. With increasing time, the temperature difference ΔT(t) and, accordingly also the reaction energy flux required to sustain the reaction, decreases.

As a parameter, the preheating time t_{PH} can be estimated using Eq. (12) assuming that the reaction propagates as soon as the ignition temperature T_{Ig} is reached, i.e.

$$T_{\mathrm{Ig}} = (T_{Ig}^{'} - T_{\mathrm{In}}) \cdot \mathrm{erfc}\left(\frac{l/2}{2\sqrt{D_{\mathrm{R}} \cdot t_{\mathrm{PH}}}} \right) + T_{\mathrm{In}}, \tag{12}$$

Eq. (12) is fulfilled for:

$$\mathrm{erfc}\left(\frac{l/2}{2\sqrt{D_{\mathrm{R}} \cdot t_{\mathrm{PH}}}} \right) = 1 - \varepsilon. \tag{13}$$

Eq. (13) is solved for $\varepsilon = 0.01$ (and therefore $T'_{\mathrm{Ig}} = T_{\mathrm{Ig}} + 0.01(T_{\mathrm{Ig}} - T_{\mathrm{In}})$) and the preheating time t_{PH} is entered into Eq. (11) in order to calculate the minimum reaction rate R_{tran}.

Unstable reaction

For reaction rates $R < R_{\mathrm{tran}}$ the initial energy dissipates rapidly and eventually the temperature falls below the ignition temperature T_{Ig}. As a consequence, the energy output ceases unless the reaction is reinitiated by an external energy input. Unstable reactions do not self-propagate.

4. Numerical Simulation

In the following, numerical analyses on SHS are conducted. First, parametric studies on the reaction parameters scaled ignition temperature $T_{\mathrm{Ig}} - T_{\mathrm{In}}$, volumetric reaction rate R and reaction zone thickness l are addressed. In the second part of the numerical analysis, typical reaction parameters for NiAl formation are assumed and the impact of different joining materials on reaction stability and velocity is investigated. In order to limit the complexity of this analysis, only one parameter is varied at any one time. If not mentioned otherwise, the following standard values are defined: reaction zone thickness $l = 100$ µm, scaled ignition temperature $T_{\mathrm{Ig}} - T_{\mathrm{In}} = 290$ K.

4.1 Reaction parameters

In this part of the numerical analysis, the impact of the reaction parameters on SHS is considered. In all cases, the material properties correspond to NiAl. The reaction parameters include the reaction zone thickness, the scaled ignition temperature and the reaction rate.

Reaction zone thickness

First, let us consider the reaction zone thickness. A total of seven models with thicknesses l = 5, 10, 25, 50, 100, 200, 300 µm are considered. In Figure 3, the minimum reaction rate R_{min} and corresponding minimum propagation velocity v_{min} is plotted versus thickness l. It can readily be seen that for very thin reaction zones (i.e. $l < 50$ µm) high reaction rates are required. The reason is the very short conduction length $l/2$ out of the reaction zone into the adjacent material for the thermal energy. In order to compensate for this fast energy transfer, high reaction rates are required. For most relevant intermetallic reactions, such high reaction rates cannot be achieved, i.e. self-propagating reactions are not possible. Increasing the thickness l distinctly decreases the required rate to more feasible values such as 41.5 W·mm^{-3} (l = 300 µm). In addition to the FE results, the minimum reaction rates R_{stat} and R_{tran} for self-propagation are estimated using Eqs. (6) and (11). Equation (6) distinctly overestimates the required energy flux since it does not account for the preheating of the reaction zone. In contrast, Eq. (11) enables a particularly accurate estimation of R_{min}. Figure 3 also shows the minimum propagation velocity v_{min}. This velocity is closely linked to the minimum reaction rate: higher rates correspond to fast conductive heat transfer (from the reaction zone) and thus a faster propagation of the reaction.

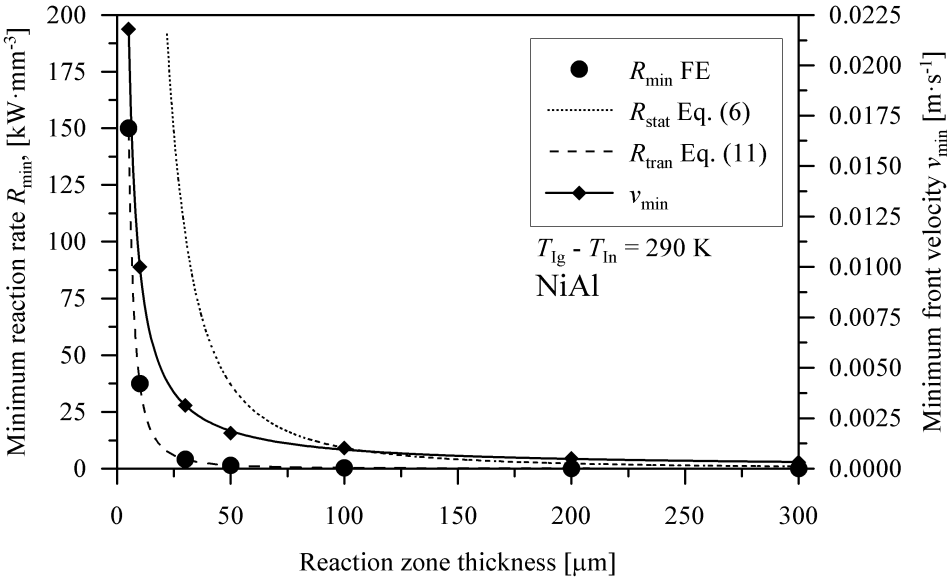

Figure 3 Parametric study of the reaction zone thickness.

Reaction rate

Next, the influence of the reaction rate R on SHS is considered. The reaction rate strongly depends on the considered intermetallic reaction (for example NiAl formation) and temperature. The increase of the reaction rate with temperature can be estimated using the Arrhenius equation:

$$R(T) \cdot V = F \cdot e^{\frac{-E_a}{R_G \cdot T}}, \tag{14}$$

where E_a is the activation energy, R_G is the gas constant and F is a pre-exponential factor.

It has been demonstrated in the previous section that a minimum reaction rate R_{min} is required to achieve self-propagation. An increase of R beyond this threshold causes additional energy release resulting in elevated temperatures and accelerated heat transfer into the adjacent reaction zone. As a result, the propagation velocity v is increased. In the following analysis, two reaction zone thicknesses l = 50, 100 μm are considered and the scaled ignition temperature $T_{Ig} - T_{In}$ is constant at 290 K. The results of the parametric study are shown in Fig. 4. It can be seen that the propagation velocity increases with the reaction rate. The dependence can be expressed as a parabolic function $v(R) = a \cdot R^2 + b \cdot R + c$ for $R > R_{min}$. The corresponding parameters are a = -0.0002, b = 0.017, c = -0.014 (l = 50 μm) and a = -0.0004, b = 0.0265, c = 0.0002 (l = 100 μm).

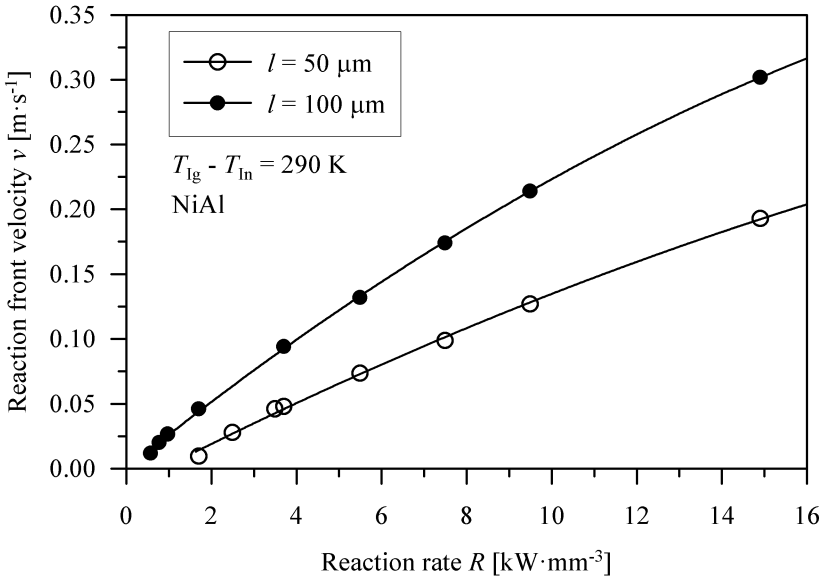

Fig. 4 Parametric study of the reaction rate.

Scaled ignition temperature

The scaled ignition temperature T_{Ig} - T_{In} determines of course the ability to overcome the activation energy of the reaction. As a consequence, it is an important parameter for reaction stability and propagation velocity. The ignition temperature depends on the reaction considered and generally cannot be altered. However, by preheating of the joining components the initial temperature can be increased and thus the temperature difference $T_{Ig} - T_{In}$ can be decreased. Analysis of Eqs. (6) and (11) reveals that the minimum required reaction rate R_{min} decreases for increasing values of the initial temperature T_{In}. Furthermore, Fig. 4 indicates that for reaction rates $R > R_{min}$ the reaction front velocity v is increased. As a consequence, an increase of the initial temperature T_{In} increases the reaction front velocity.

In Fig. 5*a* the minimum rate R_{min} is plotted versus the scaled ignition temperature $T_{Ig} - T_{In}$. As predicted by Eqs. (6) and (11), the minimum rate decreases for smaller scaled ignition temperatures. The relation can be expressed by a linear function of the form: $R_{min}(\Delta T) = a \cdot \Delta T$. The corresponding parameters are a = 5.21 W·mm^{-3}·K^{-1} (l = 50 µm) and a = 1.31 W·mm^{-3}·K^{-1} (l = 100 µm). In addition to the numerical results, R_{tran} is calculated using Eq. (11). Again, excellent agreement with the numerical data is found.

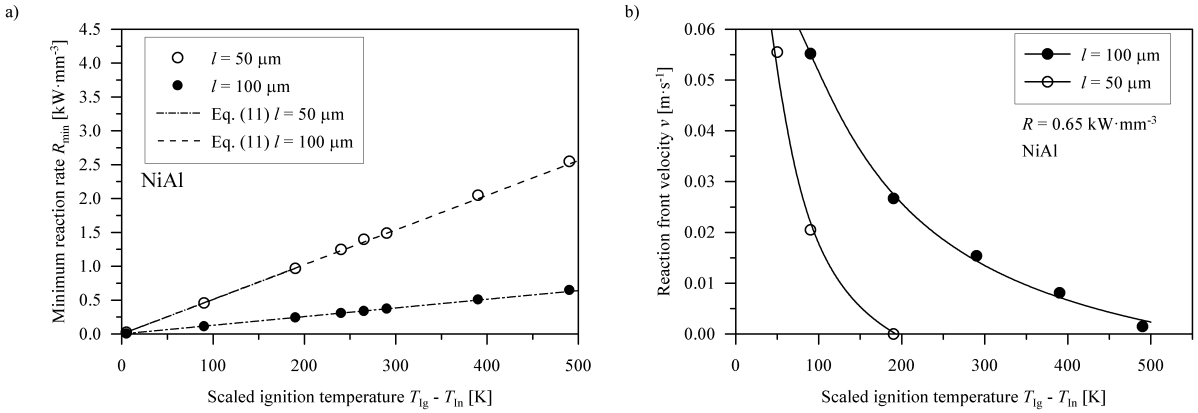

Fig. 5 Study of the scaled ignition temperature: a) minimum reaction rate, b) reaction front velocity.

Next, the propagation velocity v is investigated for the constant reaction rate R = 0.65 kW·mm^{-3}. Results are plotted in Fig. 5*b* versus the scaled ignition temperature. Two thicknesses l = 50, 100 μm are considered. For the given reaction rate and the reaction zone l = 50 μm, self-propagation only occurs for $T_{Ig} - T_{In} < 200$ K. In both cases, decrease of the scaled ignition temperature causes a rapid increase of the reaction front velocity v. It can be concluded that preheating of joining components and reaction zone is an efficient way to ensure reaction stability and increase the propagation velocity v.

4.2 Material properties

In the final part of the numerical analysis, the influence of material properties on SHS in joining operations is considered. In all cases, the material properties of the reaction zones correspond to NiAl. We simulated the self-joining of the following materials: the intermetallic NiAl and the two amorphous alloys $Mg_{60}Cu_{40}Y_{10}$ and $Pd_{40}Ni_{40}P_{20}$. All material properties are listed in Table 1.

Material	**Conductivity λ** [W·m^{-1}·K^{-1}]	**Specific heat C** [J·kg^{-1}·K^{-1}]	**Density ρ** [kg·m^{-3}]	**Thermal diffusivity D** [m^2·s^{-1}]
NiAl	80	630	5850	2.17E-5
$Mg_{60}Cu_{40}Y_{10}$	235	712	3130	1.05E-4
$Pd_{40}Ni_{40}P_{20}$	7.03	346	9415	2.16E-6

Table 1: thermal material properties [14-16]

The results of the analysis are shown in Fig. 6. The propagation velocity v is plotted versus the reaction rate for the standard reaction parameters ($T_{Ig} - T_{In}$ = 290 K and l = 100 μm). For comparison, the NiAl results are taken from Fig. 4 and added as a dotted line. The results for $Mg_{60}Cu_{40}Y_{10}$ and $Pd_{40}Ni_{40}P_{20}$ are shown as drawn lines and triangular and circular markers, respectively. The amorphous alloy $Pd_{40}Ni_{40}P_{20}$ exhibits a low thermal diffusivity D / conductivity λ and, accordingly, a relatively slow reaction rate R_{min} = 0.035 kW·mm^{-3} is sufficient for SHS. In comparison, the $Mg_{60}Cu_{40}Y_{10}$ alloy is a good thermal conductor (i.e. has a high thermal diffusivity and conductivity) and self-propagation is only achieved at reaction rates R_{min} = 1.2 kW·mm^{-3}. These values indicate that depending on their thermal properties not all amorphous alloys may be suitable for SHS joining operations. For good thermal conductors, self-propagation requires high reaction rates that could well exceed those of commonly available SHS reactions. However, the above parametric studies indicate possibilities to extend the applicability of SHS joining: the minimum reaction rate can be lowered by the pre-heating of the components to be joined and/or an increase of the reaction zone thickness.

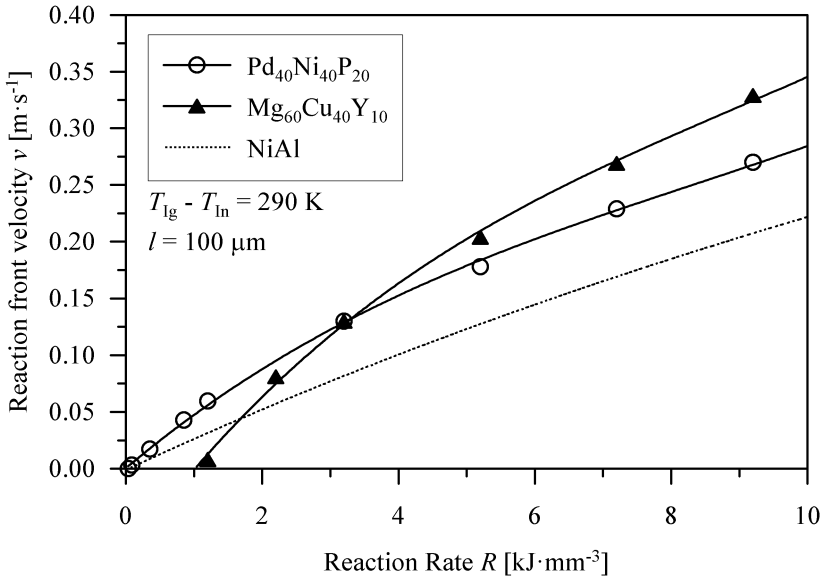

Fig. 6 Reaction front velocities for joining of amorphous alloys.

Figure 7 shows the transient temperature profile of the reaction zone and adjacent joining material. The two amorphous alloys $Mg_{60}Cu_{40}Y_{10}$ and $Pd_{40}Ni_{40}P_{20}$ are considered. In both cases, the thickness l of the reaction zone is 300 µm and the scaled ignition temperature is 290 K. The reaction rate R is 3.2 kW·mm^{-3} so that the reaction front velocity is identical v = 0.13 m·s^{-1} (see Fig. 6). Temperatures are plotted in the centre of the reaction zone and at control points located on a line perpendicular to the reaction zone in intervals l = 300 µm.

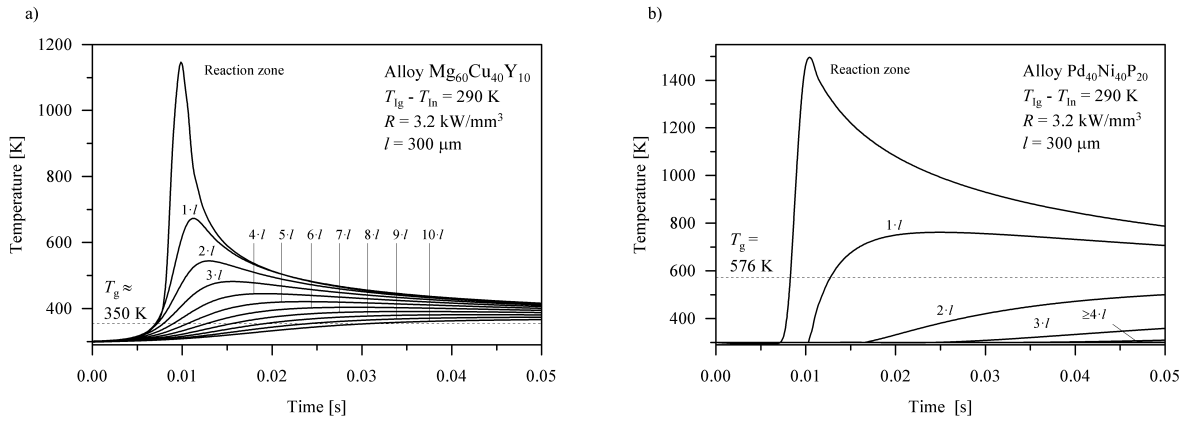

Fig. 7 Transient temperature profile during the SHS reaction.

Initially, all measurement points are at T_{In} = 300 K. As the SHS front approaches the measurement line, the temperature inside the reaction zone rapidly increases. The maximum temperature is T = 1515 K for $Pd_{40}Ni_{40}P_{20}$ and T = 1170 K for $Mg_{60}Cu_{40}Y_{10}$. The deviation is caused by the different thermal diffusivities (see Table 1) of the two amorphous alloys. $Pd_{40}Ni_{40}P_{20}$ exhibits a low thermal diffusivity and, accordingly, the thermal energy is mostly contained within close proximity to the reaction zone thus resulting in locally elevated temperatures. At a distance $d = 1 \cdot l$ from the reaction zone temperatures still extend up to 760 K. However, with increasing distance $d \geq 4 \cdot l$ the temperature in the amorphous alloy is hardly affected by the SHS. In comparison, in the highly conducting In $Mg_{60}Cu_{40}Y_{10}$ alloy, energy is rapidly conducted away from the reaction zone resulting in lower maximum temperatures. On the downside, the heat-affected area of the amorphous alloy is much larger and even at a distance $d = 10 \cdot l$ a distinct temperature increase is observed.

In order to evaluate the impact of the joining operation on the amorphous alloys the glass transition temperature T_g of each material must be considered. It has been reported in Inoue et al. [16] that the compressive 0.2% yield stress of $Mg_{60}Cu_{40}Y_{10}$ remains unchanged up to 350 K and significantly decreases at higher temperatures. Based on this data, it can be concluded that the strength of the material to be joined is distinctly decreased up to a distance of $d = 10 \cdot l = 3$ mm (total thickness is 6 mm). In He et al. [17] the glass transition temperature of $Pd_{40}Ni_{40}P_{20}$ is given as $T_g = 576$ K. Accordingly, only the material directly adjacent to the reaction zone is affected by the SHS. The temperature at $d \geq 2 \cdot l = 0.6$ mm is significantly lower than T_g and accordingly no crystallization of the amorphous alloy would be expected.

5. Conclusions

A parametric study of self-propagating high temperature synthesis (SHS) in joining operations of temperature sensitive materials (i.e. amorphous alloys) has been conducted. Within this context, SHS must generate sufficient thermal energy to self-propagate but simultaneously thermal energy transfer to the adjacent amorphous alloys must be minimised in order to avoid crystallization of the material. Analytical estimations for the minimum reaction rates required for self-propagation have been developed and compared to finite element simulations. Good agreement was found. The parametric studies indicate that both reaction stability and propagation velocity can be increased by preheating of the components to be joined or by increasing the thickness of the reaction zone. The propagation velocity was also found to increase for higher reaction rates. Finally, a case study for the joining of the intermetallic NiAl and the amorphous alloys $Mg_{60}Cu_{40}Y_{10}$ and $Pd_{40}Ni_{40}P_{20}$ was conducted. The minimum reaction rate was found to increase with the thermal diffusivity of the joining material. The results indicate that good thermal conductors require very high reaction rates that may exceed those of commonly available SHS reactions. Furthermore, a strong dependence of the transient temperatures in proximity of the reaction zone was found. The results show that the effectiveness of SHS for the joining of amorphous alloys strongly depends on the material, in particular its thermal diffusivity D and glass transition temperature T_g. A high thermal diffusivity of the amorphous alloy increases the heat affected area but simultaneously decreases absolute temperatures due to the rapid energy dissipation. In the case of a low thermal diffusivity, the temperature affected zone is smaller but high temperatures occur that are likely to exceed the glass transition temperature.

Acknowledgements

We wish to thank the ARC for their generous support of this research under the Discovery Project Grants Scheme.

References

[1] J. J. Moore, H. J. Feng, Combustion synthesis of advanced materials: Part I. Reaction parameters, Prog. Mater. Sci. 39 (1995) 243-275.

[2] T. P. Weihs, Self-propagating reactions in multilayer materials, in: G.A. Glocker, S.I. Shah (Eds.), Handbook of thin film process technology, IOP, Bristol, 1998.

[3] I. E. Gunduz, K. Fadenberger, M. Kokonou, C. Rebholz, C. C. Doumanidis, Investigations on the self propagating reactions of nickel and aluminum multilayered foils, Appl. Phys. Letters 93 (2008) 134101.

[4] Y. Kawamura, Y. Ohno, A. Chiba, Development of Welding Technologies in Bulk Metallic Glasses, Mater. Sci. Forum 386 (2002) 553-558.

[5] A. Inoue, Bulk amorphous alloys-practical characteristics and applications ,TTP, Materials Science Foundations, Zürich, 1999.

[6] H. Z. Hu, S. N. Ma, X. R. Chen, Structure and properties investigation about a Copper-base SHS welding material, Key Eng. Mat. 373 (2008) 505-508.

[7] C. Pascal, R. M. Marin-Ayral, J. C. Tédenac, Joining of nickel monoaluminide to a superalloy substrate by high pressure self-propagating high-temperature synthesis, J. Alloy Compd. 337 (2002) 221-225.

[8] I. E. Gunduz, K. Fadenberger, M. Kokonou, C. Rebholz, C. C. Doumanidis, T. Ando, Modeling of the self-propagating reactions of nickel and aluminium multilayered foils, J. Appl. Phys. 105 (2009) 074903-1-074903-9.

[9] O. S. Rabinovich, P. S. Grinchuk, M. A. Andreev, B. B. Khina, Conditions for combustion synthesis in nanosized Ni/Al films on a substrate, Physica B 392 (2007) 272-280.

[10] E. V. Levchenko, A. V. Esteev, D. P. Riley, I. V. Belova, and G. E. Murch, Molecular dynamics simulation of the alloying reaction in Al-coated Ni nanoparticle, Comp. Mater. Sci. 47 (2010) 712-720.

[11] MSC.Software Corporation, Handbook, Volume A: Theory and User Information, 2007.

[12] S. Dong., P. Hou, H. Cheng, H. Yang, and G. Zou, Fabrication of intermetallic NiAl by self-propagating high-temperature synthesis reaction using aluminium nanopowder under high pressure, J. Phys.-Condens. Mat. 14 (2002) 11023-11030.

[13] A. V. Evteev, E. V. Levchenko, D. P. Riley, I. V. Belova G. E. Murch, Reaction of Ni-coated Al nanoparticle to form B2-NiAl: A molecular dynamics study, Phil. Mag. Lett. 89 (2009) 815-830.

[14] D. B. Miracle, The Physical and Mechanical Properties of NiAl, Acta Metall. Mater. 41 (1993) 649-684.

[15] U. Harms, T. D. Shen, R. B. Schwarz, Thermal conductivity of $Pd_{40}Ni_{40-x}Cu_xP_{20}$ metallic glasses Scripta Mater. 47 (2002) 411-414.

[16] A. Inoue, A. Kato, T. Zhang, S. G. Kim, T. Masumoto, Mg-Cu-Y Amorphous Alloys with High Mechanical Strengths Produced by a Metallic Mold Casting Method, Mater. Trans. 32 (1991) 609-616.

[17] Y. He, R. B. Schwarz, J. I. Archuleta, Bulk glass formation in the Pd–Ni–P system, Appl. Phys. Lett. 69 (1996) 1861-1863.